Stability Investigation of the Quadripod Structure for the NASA/JPL 70-Meter Antenna

C. T. Chian, J. J. Cucchissi, and R. Levy
Ground Antennas and Facilities Engineering Section

A new, slim-profiled, low-blockage quadripod structure was designed to support the 7.7-m-diameter subreflector for the 70-m antenna. Detailed analyses of quadripod structural stability (in frequency and buckling) are presented. The results indicate that the new quadripod design has an adequate safety margin for buckling, and its lowest natural frequency is above the control system bandwidth. The analytical design frequencies were confirmed by actual field measurements made in Spain in February 1986.

I. Introduction

The upgrade of the three NASA/JPL 64-m diameter antennas will provide a needed increase in Earth-based space communication capability at all three Deep Space Communications Complexes: Goldstone, California (DSS 14); Canberra, Australia (DSS 43); and Madrid, Spain (DSS 63). In addition to the increase of the antenna aperture area from 64 m to 70 m, a number of significant improvements in the quadripod, surface panels, subreflector positioner, and microwave aspects are included in the design. The upgrade objective is to increase the radio-frequency (RF) gain/noise temperature (G/T) by about 1.9 dB at X-band (8.45 GHz).

As part of the upgrade effort, a new, high-precision 7.7-m (25.4-ft)-diameter subreflector and positioning mechanism are needed. Consequently, an entirely new quadripod structure is required to support the subreflector. The new quadripod design particularly emphasizes reduced RF blockage, which is achieved by means of a narrow cross-sectional profile of the legs. The profile adopted provides about 0.32 dB of gain improvement in comparison with the existing 64-meter design (Ref. 1). This report addresses the stability analyses performed on the new quadripod design to ensure that it has an adequate safety margin for buckling and that the minimum natural frequency is compatible with control system requirements.

After construction, full-scale vibration measurements were performed at the fabricator's plant on the completed and assembled structure with dummy weights to simulate the subreflector and other equipment loads.

II. Design

The quadripod assembly is a tabular space-frame steel structure with four trapezoidally shaped legs connected to another large space frame at the apex, as shown in Figs. 1 and 2. The four legs are supported at the corner points of the rectangular truss system of the main reflector structure as shown in Fig. 2. The final slim profile leg cross-section enve-

lope selected is shown in Fig. 3. Also, the quadripod will be used occasionally for hoisting the cassegrain feed cones, the subreflector, or other heavy equipment which may be removed and reinstalled.

The finite element model of the 70-m quadripod truss structure is a pin-joined frame (3 translational degrees of freedom per node) comprising 156 nodes, 445 axial bars, and 28 membrane plates. The JPL/IDEAS (Iterative Design of Antenna Structures) computer program was used for analysis and design (Ref. 2). The program employs the optimality criterion to minimize the structural weight (objective function) with a constraint placed on the lowest natural frequency. A subsequent analysis of the 70-m model, accounting for bending and torsional stiffness at the joints (6 degrees of freedom per node) using NASTRAN (Ref. 3), showed only a small increase in the torsional natural frequency (Ref. 1). Outrigger braces (Fig. 2) were added thereafter to increase the lowest natural frequency.

Due to the slimness of the quadripod legs, the following requirements had to be considered:

(1) *Dynamic stability*. The original 64-m antenna quadripod, with a minimum natural frequency of 1.22 Hz, presented no control system stability problems. Therefore, it was recommended that the minimum natural frequency of the new 70-m antenna quadripod must be 1.22 Hz. There are several distinct types of vibration modes characteristic of quadripod structures. Torsional modes can be excited at near-zenith antenna elevation by the azimuth drive. Lateral vibration cantilever modes can be excited by the azimuth drive at low elevation angles, and cantilever pitch modes can be excited by the elevation drive at any elevation angle, as shown in Fig. 4.

    The torsional mode had the lowest frequency, so this frequency was selected as the primary design constraint. It was also found that this frequency could be significantly increased by adding outrigger braces near the quadripod base. These braces have an important stiffening effect and provide an insignificant increase in blockage. However, the braces are attached to an elastic antenna structure, and the compliance of this structure could reduce the outrigger contribution to the stiffness of the quadripod. Therefore, the consequences of partially effective outrigger braces on natural frequency were also studied.

(2) *Static buckling stability*. The occasional use of the quadripod as a derrick required a check on the possibility of buckling instability. A factor of safety of at least 1.5 was recommended. The smallest eigenvalue found from a structural buckling analysis is equivalent to this factor of safety. Since the IDEAS program that was used for design and natural frequency analyses does not perform buckling analysis, the new quadripod design was optimized for the frequency requirement using IDEAS and then analyzed for buckling using NASTRAN (NASA Structural Analysis Program). NASTRAN was used to determine the buckling loads of the natural frequency-constrained quadripod design. Two versions of the NASTRAN program were used because of possible different finite element formulations: the NASTRAN-COSMIC (NASA's *C*omputer *S*oftware *M*anagement and *I*nformation *C*enter) (Ref. 4) and the proprietary NASTRAN-MSC version (MacNeal-Schwendler Corporation) (Ref. 3). The two versions were used both for the buckling and natural frequency analyses, and the results obtained were compared.

III. Natural Frequency Analysis and Results

For natural frequency and mode shape analysis, the IDEAS program uses the Simultaneous Iteration method (Ref. 5), which is an iterative extension of Guyan's one-step solution. The NASTRAN programs in this study used the conventional Inverse Power Method.

Table 1 compares the first three natural frequencies of two pin-joined quadripod models; one with outrigger braces and the other without braces. All the values of Table 1 (except mode 1 without outriggers) exceed the goal of 1.22 Hz. Despite their effect on frequency, the braces do not significantly alter the characterization of the mode shapes of interest: the lowest mode is torsional and the next lowest are lateral and pitch cantilever modes. This table makes it evident that the outriggers are effective and approximately double the lowest frequency. Also included in Table 1 are the field measurements made on the assembled quadripod (Ref. 6).

To study the consequences of varying degrees of outrigger fixity caused by partially effective braces, the axial stiffness of the outriggers was parameterized, and the resulting natural frequencies were computed and plotted in Fig. 5. This approach is equivalent to reducing the "stiffness" of the support points. There is a relatively small change in frequency as long as the stiffness is at least 50% of the maximum. This fortuitous condition results from the requirement that the quadripod supports the hoisting loads.

IV. Results of Buckling Analysis

The Rigid Format No. 5 of the NASTRAN program was used to perform the buckling analysis. The results of the

buckling analysis for the quadripod pin-joined model are presented in Table 2. Both the COSMIC and MSC versions of the NASTRAN program were used and compared. Four antenna configurations, each subject to the maximum loads anticipated to be hoisted when employing the quadripod as a derrick, in addition to the quadripod weight, were considered in the quadripod buckling analysis:

(1) Zenith look with outriggers.

(2) Zenith look without outriggers.

(3) Horizon look with outriggers.

(4) Horizon look without outriggers.

Table 2 shows that similar to effects on natural frequency the outriggers tend to at least double the buckling load capability.

V. Finite Element Plate Stiffness Representation

Comparisons of the COSMIC-NASTRAN and MSC-NASTRAN results on the quadripod model in Table 1 show that the plate element CQDMEM2 in the COSMIC version gives a different stiffness matrix representation compared with the CQUAD4 plate element in the MSC version, or with the IDEAS plate element CQDMEM. The lowest natural frequency of the quadripod, for instance, was found to be 1.54 Hz for the COSMIC model, while the MSC and IDEAS models gave 1.30 Hz. Table 3 compares the quadripod natural frequency results by the three computer programs: IDEAS, NASTRAN-COSMIC, and NASTRAN-MSC.

A parametric study was conducted to readjust the moduli of elasticity of the COSMIC CQDMEM2 plate elements to produce results similar to those of the MSC elements. Comparison of the results of the stiffness parameterization study is shown in Table 4 for the quadripod natural frequency analysis and in Table 5 for the quadripod buckling analysis. The plate element used in the NASTRAN-COSMIC employs the constant stress formulation, while the elements used in the NASTRAN-MSC or IDEAS permit a stress variation. As a result, the COSMIC element generates a stiffer structure than the other elements.

VI. Summary

A natural frequency and structural stability study was conducted for the 70-m antenna quadripod. The quadripod was found to be adequate in natural frequency and stable in buckling when the outrigger braces were included. One computer program used in the investigation was found to give an over-estimate of the stiffness. In order to correct the excessive stiffness, a parametric study was conducted to derive empirical coefficients to adjust the plate stiffness for future use of this program. The predicted values of natural frequency were shown to be closely consistent with actual full-scale field tests.

References

1. Cucchissi, J. J., "A New 70-Meter Antenna Quadripod With Reduced RF Blockage," *TDA Progress Report 42-82*, pp. 24-30, Jet Propulsion Laboratory, Pasadena, CA, Aug. 15, 1985.

2. Levy, R., and Chai, K., "Implementation of Natural Frequency Analysis and Optimality Criterion Design," *Computers and Structures*, Vol. 10, pp. 277-282, Pergamon Press Ltd., Great Britain, 1979.

3. McCormick, C. W., Editor, *MSC/NASTRAN User's Manual*, MSR 39, The MacNeal-Schwendler Corporation, 1983.

4. *The NASTRAN Theoretical Manual (level 15.5)*, NASA SP-221 (06), Scientific and Technical Information Office, NASA, Wash. DC, Jan. 1981.

5. Levy, R., *Guyan Reduction Solutions Recycled for Improved Accuracy*, NASA TMX-2378, Vol. 1, pp. 201-220, Sept. 1971.

6. "Vibration Measurements of Quadripod and Apex Structure for 70M Antenna DSS-63," Report No. J-K 5391, Kinemetrics, Inc., Pasadena, CA, May 1986.

Table 1. Comparison of natural frequencies for 70-m quadripod

Mode	Frequency, Hz				Predominant mode shape
	With outrigger braces		Without outrigger braces		
	Analytical	Field measurement	Analytical	Field measurement	
1	1.302	1.27	0.637	0.70	Torsion
2	1.967	1.76	1.293	1.36	Lateral cantilever
3	2.720	2.62	1.555	1.74	Pitch cantilever

Table 2. The quadripod buckling analysis results

Case	Antenna configuration	NASTRAN COSMIC version	NASTRAN MSC version
1	Zenith look, with outriggers	22.81	12.27
2	Zenith look, without outriggers	9.23	(not run)
3	Horizon look, with outriggers	12.87	3.77
4	Horizon look, without outriggers	4.12	1.66

Table 3. Comparison of lowest natural frequencies of the 70-m quadripod with outrigger braces

Mode	Frequency, Hz		
	Computer program		
	IDEAS	MSC-NASTRAN	COSMIC-NASTRAN
	Plate element		
	CQDMEM	CQUAD4	CQDMEM2
1	1.302	1.304	1.542
2	1.967	1.967	2.089
3	2.720	2.720	3.216

Table 4. Comparison of the plate element stiffness and the lowest quadripod natural frequencies

Program	Plate element	Young's modulus, N/m^2 (psi)	Shear modulus, N/m^2 (psi)	Mode 1 min. freq., Hz	Mode 2 min. freq., Hz
NASTRAN-MSC	CQUAD4	20.0×10^{10} (29.0×10^6)	8.3×10^{10} (12.0×10^6)	1.304	2.720
NASTRAN-COSMIC	CQDMEM2	14.5×10^{10} (21.0×10^6)	6.0×10^{10} (8.7×10^6)	1.312	2.737

Table 5. Comparison of the plate element stiffness and the smallest eigenvalues for the quadripod buckling analysis

Program	Plate element	Young's modulus, N/m^2 (psi)	Shear modulus, N/m^2 (psi)	λ_{min}
(a) Zenith Look Antenna Configuration, with Outrigger Braces:				
NASTRAN-MSC	CQUAD4	20.0×10^{10} (29.0×10^6)	8.3×10^{10} (12.0×10^6)	12.27
NASTRAN-COSMIC	CQDMEM2	10.7×10^{10} (15.5×10^6)	4.4×10^{10} (6.4×10^6)	12.30
(b) Horizon Look Antenna Configuration, with Outrigger Braces:				
NASTRAN-MSC	CQUAD4	20.0×10^{10} (29.0×10^6)	8.3×10^{10} (12.0×10^6)	3.77
NASTRAN-COSMIC	CQDMEM2	5.2×10^{10} (7.5×10^6)	2.2×10^{10} (3.2×10^6)	3.97

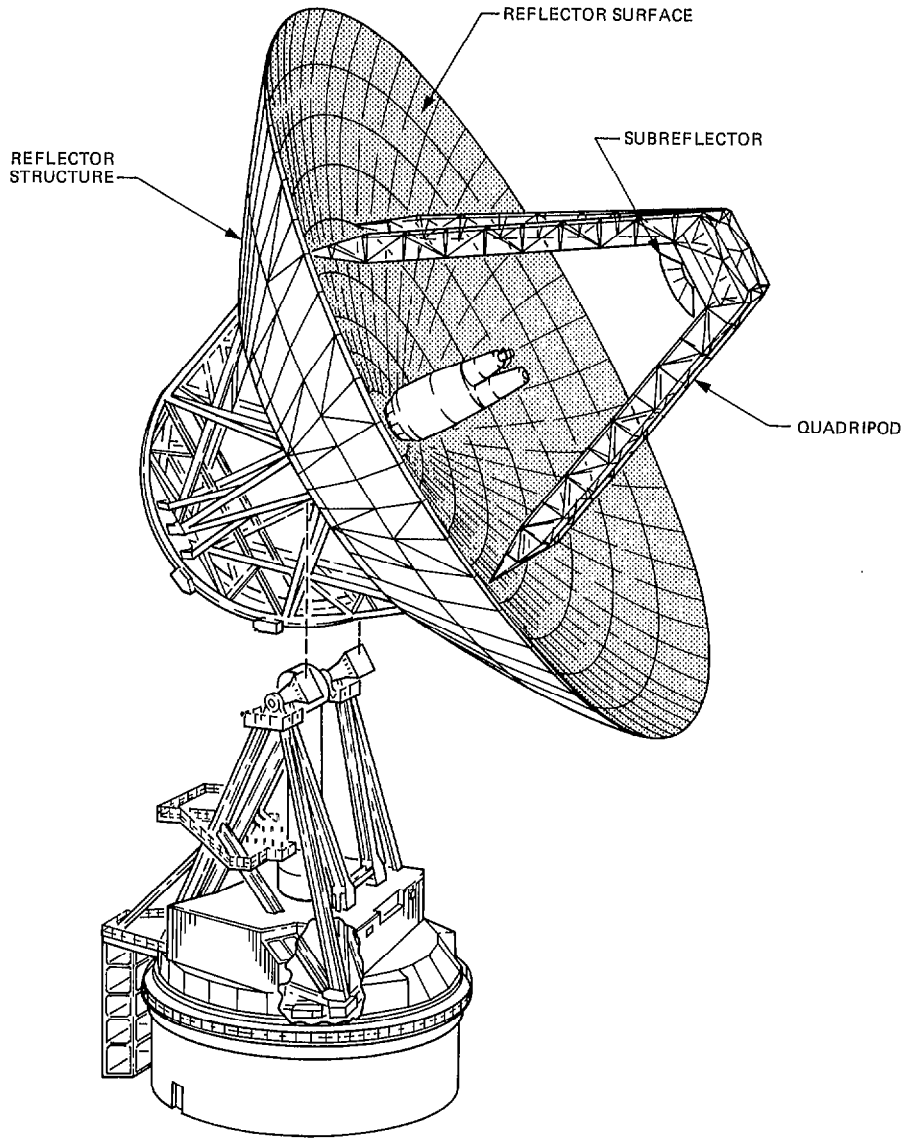

Fig. 1. Antenna quadripod and reflector system

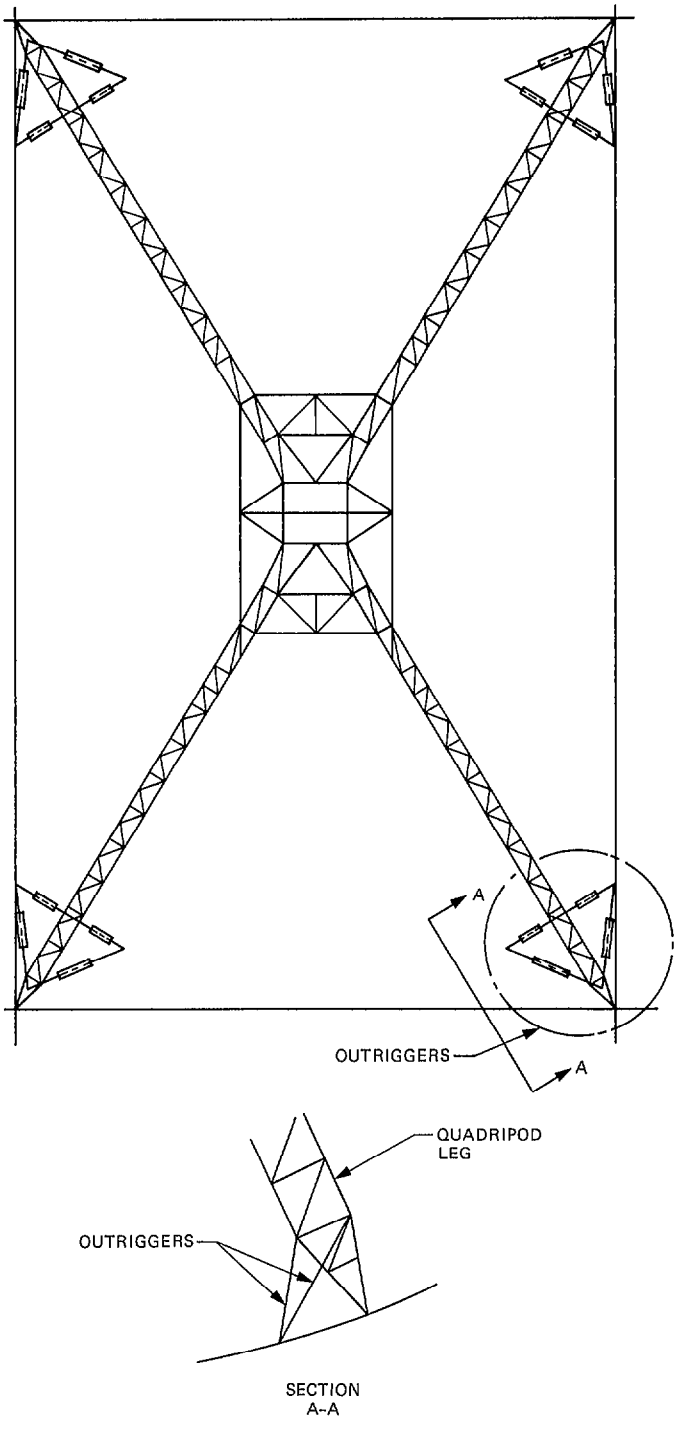

Fig. 2. Plan view of 70-m quadripod with outriggers

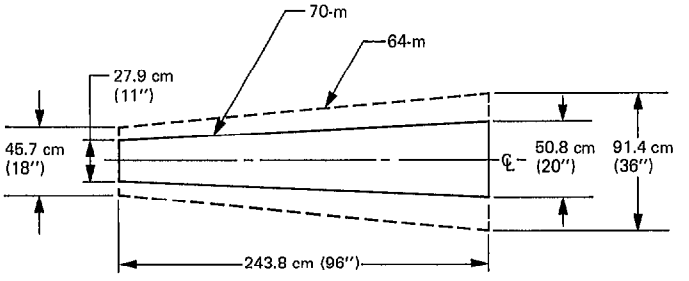

Fig. 3. Quadripod cross-sectional profile

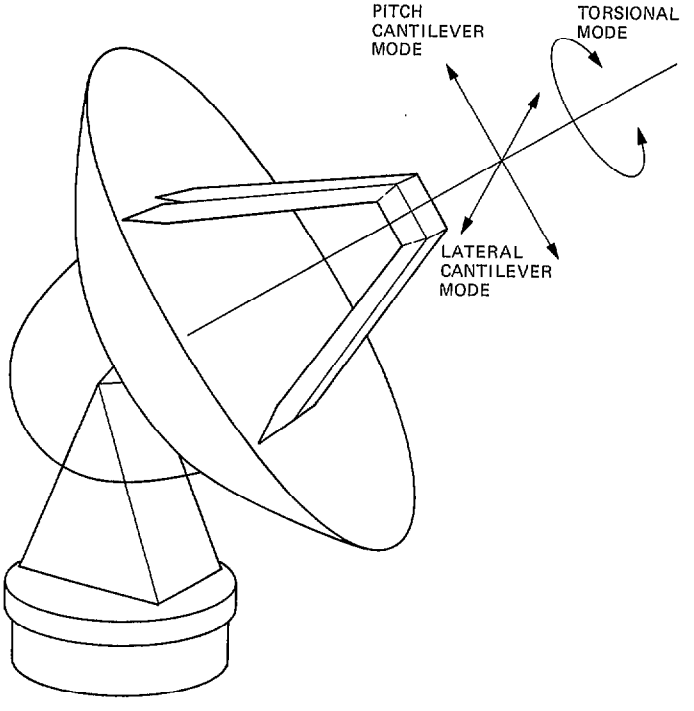

Fig. 4. Quadripod vibration modes

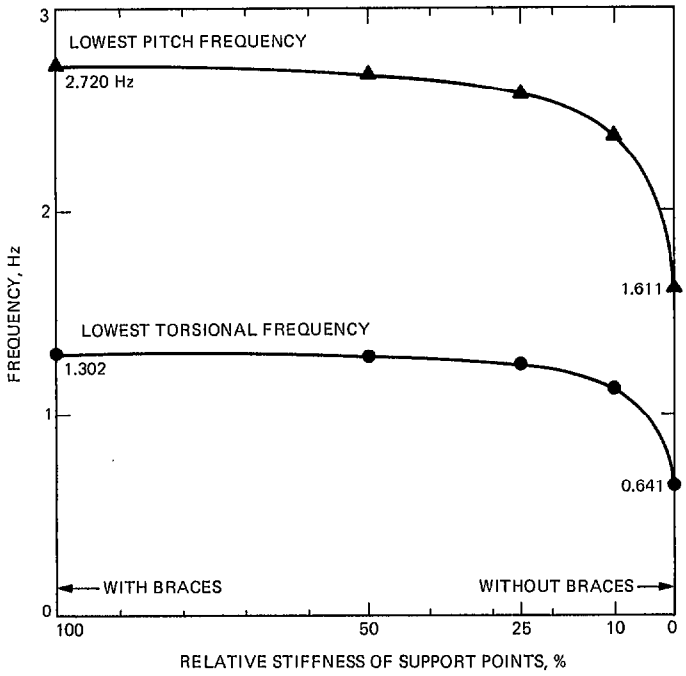

Fig. 5. Effect of outrigger braces on natural frequency

Appendix A

Differential Stiffness Matrices for Geometric Nonlinear Problems

For completeness of the report, the following material, which is extracted from Ref. 3, is included to describe formulation of the differential stiffness matrix that is used in the buckling analysis. The differential stiffness approximation uses terms up to quadratic in the strain-displacement relationship. The linear elastic solution and the differential stiffness solution are the first two iterations in the geometric nonlinear algorithm, which is an iterative technique that utilizes a modified Newton–Raphson method.

The approach requires a "Displaced Element Coordinate System" to be constructed for each element, which follows and rotates with the element as the model deforms. In the displaced element coordinate system, the distortions are small, and linear elastic theory can be used. Element forces in the displaced element coordinate system are computed by simply premultiplying the displacements by the elastic (small motion) stiffness matrix. The incremental stiffness matrix, when expressed in the displaced element coordinate system, is the sum of the elastic and differential stiffness matrices.

The term "differential stiffness" applies to linear terms in the equations of motion of an elastic body that arise from a simultaneous consideration of large, nonlinear motions and the applied loads.

The approach to the theory of differential stiffness is based on Lagrange's equations for the motion of a system with a finite number of degrees of freedom. Consider a system with a finite number of degrees of freedom, q_r; with a set of springs whose potential energy is V; and with a set of loads, P_a, applied to displacements u_a. The equations of motion for the system may be written

$$\frac{\partial V}{\partial q_r} = Q_r, \quad r = 1,2,3,\ldots,n \tag{A-1}$$

where the generalized force Q_r is given by

$$Q_r = \frac{\partial W}{\partial q_r} = \sum_a \frac{\partial u_a}{\partial q_r} P_a \tag{A-2}$$

W is the work done by the external forces. It is assumed in the theory of differential stiffness that the potential energy of differential stiffness is a quadratic function of the degrees of freedom, i.e.,

$$V = \frac{1}{2} \sum_{i,j} a_{ij} q_i q_j \tag{A-3}$$

but that the partial derivatives, $\partial u_a / \partial q_r$, are not necessarily constants.

The Lagrangian discrete element approach can be applied to a general elastic body, if it be imagined that the body is made up of infinitesimal cubes, each of which is joined to its six neighbors by a universal joint at the midpoint of each face. For a given static loading on the body, the stress distribution is computed throughout the body, ignoring differential stiffness effects in the process. This internal stress distribution is taken as the equivalent loading, and is applied to each cube in turn to determine the differential stiffness for the cube.

The work done by the static loads is computed for general motion of the degrees of freedom using Eq. (A-2). The terms in the differential stiffness matrix for the cube are then computed from

$$K_{rs} = -\frac{\partial Q_r}{\partial q_s} = -\frac{\partial^2 W}{\partial q_s \partial q_r} \tag{A-4}$$

The total work done by all components of force on a cube of volume Δv is

$$\Delta W = -\frac{\Delta v}{2} [\omega_x^2 (\sigma_y + \sigma_z) + \omega_y^2 (\sigma_z + \sigma_x) + \omega_z^2 (\sigma_x + \sigma_y)$$

$$-2\,\omega_x\,\omega_y\,\tau_{xy} - 2\,\omega_y\,\omega_z\,\tau_{yz} - 2\,\omega_z\,\omega_x\,\tau_{zx}] \tag{A-5}$$

where ω_x, ω_y, and ω_z are rotations about the x, y, and z axes, respectively. No work is done on the cube during translation because the forces acting on the cube are in equilibrium.

The matrix of differential stiffness coefficients for a cube of volume Δv is written from Eq. (A-4) as

$$\Delta[K^d] = \Delta v \begin{bmatrix} \sigma_y + \sigma_z & -\tau_{xy} & -\tau_{zx} \\ -\tau_{xy} & \sigma_z + \sigma_x & -\tau_{yz} \\ -\tau_{zx} & -\tau_{yz} & \sigma_x + \sigma_y \end{bmatrix} \tag{A-6}$$

The above general result is applied to evaluate the differential stiffness matrices for the quadripod structural elements.

Appendix B
Buckling Analysis Procedure

The formulation of the quadripod linear static response problem by the displacement method is described by the matrix equation

$$[\mathbf{K}] \ \{\mathbf{u}\} = \{\mathbf{P}\} \qquad \text{(B-1)}$$

where $[\mathbf{K}]$ is the stiffness matrix, $\{\mathbf{u}\}$ is the displacement vector, and $\{\mathbf{P}\}$ is the load vector.

The steps for solving a quadripod buckling problem are listed as follows:

(1) Solve the linear static response problem Eq. (B-1) for the quadripod structure in the absence of differential stiffness, and compute the internal forces in elements.

(2) Using the results of Step (1), calculate the differential stiffness matrices for individual elements, and apply the standard reduction procedures (constraints and partitioning) to form the differential stiffness matrix $[\mathbf{K}^d]$ in final form.

(3) Replace the load vector $\{\mathbf{P}\}$ by $-\lambda\,[\mathbf{K}^d]\ \{\mathbf{u}\}$, and find eigenvalues and eigenvectors for

$$[\mathbf{K} + \lambda\,\mathbf{K}^d]\ \{\mathbf{u}\} = 0 \qquad \text{(B-2)}$$

The eigenvalues, λ, are the load level factors by which the applied static loading is multiplied to produce buckling:

$$P_{cr} = \lambda P \qquad \text{(B-3)}$$

P_{cr} is the critical load for buckling, and P is the applied load.

The eigenvalues, λ_i, and the corresponding eigenvectors, $\{\phi_i\}$, are extracted by the Real Eigenvalue Analysis Module. The criterion for the qaudripod structure to be statically stable (free from buckling) is, therefore:

$$\lambda_i > 1 \qquad \text{(B-4)}$$